Appendix

Deciphering the Physiological Response of *Escherichia coli* Under High ATP Demand

Simon Boecker, Giulia Slaviero, Thorben Schramm,
Witold Szymanski, Hannes Link, Steffen Klamt*

*) correspondence: klamt@mpi-magdeburg.mpg.de

This PDF file includes:

- Supplementary Text (Detailed documentation of kinetic model)

Supplementary Text

This Supplementary Text describes the two versions of the kinetic model of the central metabolism of *E. coli* under anaerobic conditions as used in the main text. We first describe version 1 before summarizing the changes introduced in version 2 and showing the results of the metabolic control analysis obtained with version 2.

1. Kinetic model version 1

1.1 Overview

The kinetic model describes the core carbon and energy metabolism of *Escherichia coli* during the exponential growth phase under anaerobic conditions. The model contains 32 metabolites and 26 reactions and consists of the two compartments cytoplasm and external environment (Scheme S1). The following major pathways are included: glucose phosphotransferase system (PTS), glycolysis, two anaplerotic reactions (PEP carboxylase and PEP carboxykinase), left and right branch of the tricarboxylic acid (TCA) cycle active under anaerobic conditions, the main fermentative pathways (leading to the fermentation products lactate, ethanol, acetate, formate and succinate), transport reactions between cytoplasm and external environment, a biomass synthesis reaction, a NGAM reaction that accounts for non-growth associated maintenance ATP demands and finally an ATPase reaction that hydrolyses ATP into ADP and whose activity depends on the level of the overexpression of the ATPase genes. Not included were gluconeogenic reactions, the Entner-Doudoroff (ED) pathway, the glyoxylate shunt (GS) and oxidative phosphorylation as they are not relevant for anaerobic growth on glucose. Furthermore, we did not include the pentose phosphate pathway (PPP), as it has, compared to glycolysis, only relatively low flux under anaerobic conditions. However, we explicitly account for the requirement of precursors (e.g. erythrose-4-phoshphate) from the PPP by adding a stoichiometrically equivalent efflux of other metabolites contained in the model (see description of the growth rate in section 1.3). Furthermore, since the PPP was not included, the reduction equivalents NADH and NADPH were lumped in one pool (referred to as NADH), which ensures that the model accounts for overall redox balance. To reduce the size of the model, some reaction steps were partially lumped as described below.

The two models used herein were implemented and simulated with Copasi (Hoops *et al*, 2006), version 4.28, and the two model versions are available as *.cps* (Copasi) files as well as in SBML format at
https://github.com/klamt-lab/Models_E.coli_High_ATP_Demand/tree/main/Kinetic%20Model.

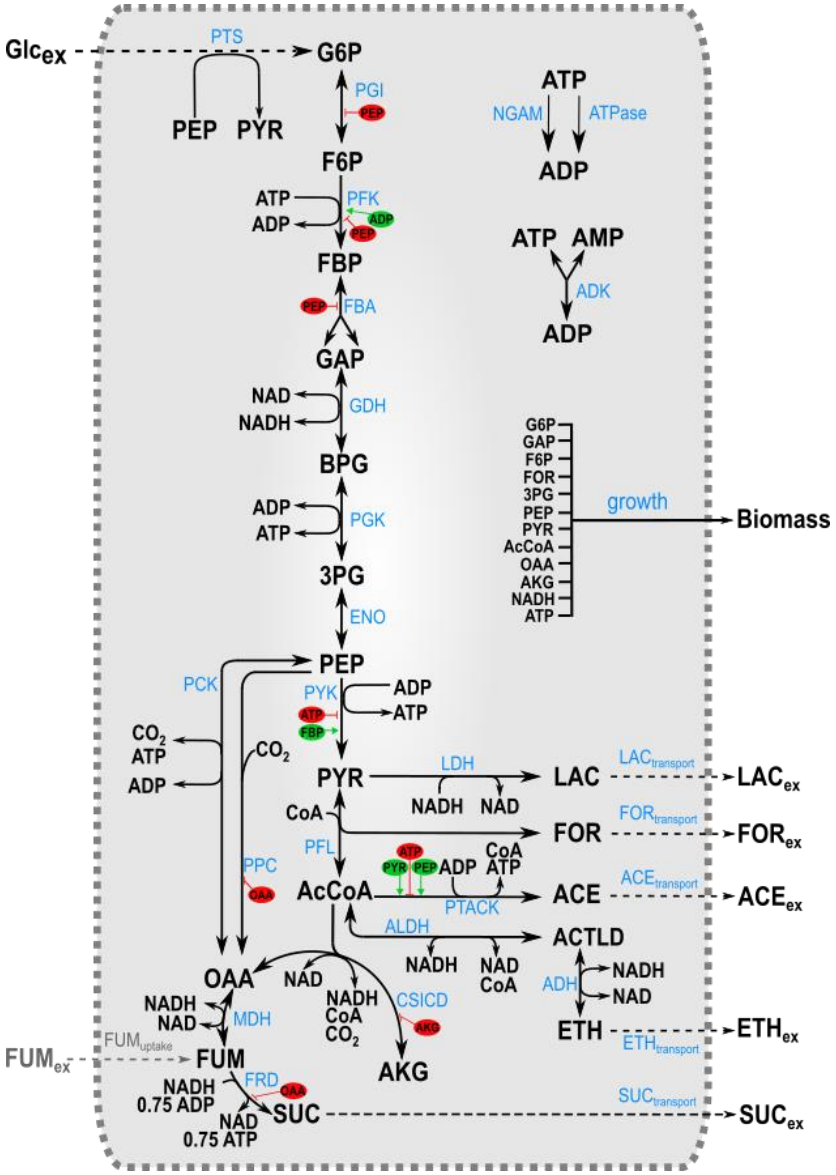

Scheme S1: Schematic of the central anaerobic carbon and energy metabolism of *E. coli* implemented in the model. Metabolites are shown in black; reactions are reported in blue and activators and inhibitors are shown in green and red, respectively. Abbreviations of metabolites and reaction names (as also used throughout this document): Glc_{ex}: external glucose (substrate); G6P: D-glucose-6-phosphate; F6P: D-fructose-6-phosphate; FBP: fructose-1,6-bisphosphate; GAP: D-glyceraldehyde-3-phosphate; BPG: 1,3-bisphospho-D-glycerate; 3PG: 3-phosphoglycerate; PEP: phosphoenolpyruvate; PYR: pyruvate; AcCoA: acetyl coenzyme A; CoA: coenzyme A; AKG: α-ketoglutarate; OAA: oxaloacetate; FUM: fumarate; SUC: succinate (intracellular); FOR: formate (intracellular); LAC: lactate (intracellular); ACE: acetate (intracellular); ACTLD: acetaldehyde; ETH: ethanol (intracellular); FOR_{ex}: formate (extracellular); ETH_{ex}: ethanol (extracellular); ACE_{ex}: acetate (extracellular); LAC_{ex}: lactate (extracellular); SUC_{ex}: succinate (extracellular); FUM_{ex}: fumarate (extracellular): this metabolite was only included when simulating co-utilization of glucose and fumarate uptake by the HC ATPase strain (see main manuscript); ATP: adenosine triphosphate; ADP: adenosine diphosphate; AMP: adenosine monosphate; NAD: lumped pool of oxidized nicotinamide adenine dinucleotide (NAD) and oxidized nicotinamide adenine dinucleotide phosphate (NADP); NADH: lumped pool of reduced nicotinamide adenine dinucleotide (NADH) and reduced nicotinamide adenine dinucleotide phosphate (NADPH); CO_2: carbon dioxide (fixed concentration). PTS: phoshotransferase system; PGI: glucose-6-phosphate isomerase; PFK: phosphofructokinase; FBA: fructose-bisphosphate aldolase (the associated reaction was lumped with the reaction of the triose-phosphate isomerase (TPI) thus yielding two molecules of GAP); GHD: glyceraldehyde-3-phosphate dehydrogenase; PGK: phosphoglycerate kinase; ENO: enolase (the reaction of this enzyme was lumped with the reaction of the phosphoglycerate mutase); PYK: pyruvate kinase; PFL: pyruvate formate-

lyase (also known as formate acteyltransferase); LDH: lactate dehydrogenase; PTACK: lumped reaction of acetate kinase and phosphate acetyltransferase; ALDH: acetaldehyde-CoA dehydrogenase; ADH: alcohol dehydrogenase; PCK: phosphoenolpyruvate carboxykinase; PPC: phosphoenolpyruvate carboxylase; CSICD: lumped reaction of citrate synthase, aconitate hydratase A, aconitate hydratase B and isocitrate dehydrogenase; MDH: lumped reaction of malate dehydrogenase and fumarase; FRD: lumped reaction of fumarate reductase and of other reactions involved in fumarate reduction; $SUC_{transport}$: succinate excretion; $LAC_{transport}$: lactate excretion; $FOR_{transport}$: formate excretion; $ACE_{transport}$: acetate excretion; $ETH_{transport}$: ethanol excretion; growth: biomass synthesis reaction (its rate will be indicated with μ); NGAM: non-growth associated ATP maintenance; ATPase: reaction that hydrolyses ATP to ADP reflecting the ATPase in the different ATPase strains; ADK: adelylate kinas. Orthophosphate, water, and protons are not shown since these compounds are not explicitly considered in the model. FUM_{uptake}: fumarate uptake (this reaction was only included when simulating co-utilization of glucose and fumarate uptake by the HC ATPase strain (see main manuscript)).

1.2 Mass balances and differential equations

The unit for concentrations of internal metabolites is [μmol/gDW] (DW: dry weight) whereas [g/L] is used for external metabolites (substrates and products). Units of measured internal metabolite concentrations and of some known parameters (from databases, literature etc.) given in molar concentrations were converted to [μmol/gDW] by considering a cytosolic density of 564 $\frac{g_{DW}}{L}$ as reported in (Chassagnole *et al*, 2002). Internal metabolic fluxes are given in [μmol/gDW/s] and converted to volumetric fluxes [g/L/s] for exchange reactions of external metabolites by using the molecular weight ([g/mol]) of the respective compound.
The differential equations given below (and the reactions shown in Scheme S1) do not account for phosphate, water and protons since these compounds are not explicitly considered in the model.

$$\frac{d[\mathrm{Biomass}]}{dt} = [\mathrm{Biomass}] \cdot \mu$$
$$\frac{d[\mathrm{Glc_{ex}}]}{dt} = -\nu_{PTS} \cdot \frac{[\mathrm{Biomass}] \cdot MW_{Glucose}}{10^6}$$
$$\frac{d[\mathrm{FOR_{ex}}]}{dt} = \nu_{FOR,transport} \cdot \frac{[\mathrm{Biomass}] \cdot MW_{FOR}}{10^6}$$
$$\frac{d[\mathrm{ACE_{ex}}]}{dt} = \nu_{ACE,transport} \cdot \frac{[\mathrm{Biomass}] \cdot MW_{ACE}}{10^6}$$
$$\frac{d[\mathrm{ETH_{ex}}]}{dt} = \nu_{ETH,transport} \cdot \frac{[\mathrm{Biomass}] \cdot MW_{ETH}}{10^6}$$
$$\frac{d[\mathrm{LAC_{ex}}]}{dt} = \nu_{LAC,transport} \cdot \frac{[\mathrm{Biomass}] \cdot MW_{LAC}}{10^6}$$
$$\frac{d[\mathrm{SUC_{ex}}]}{dt} = \nu_{SUC,transport} \cdot \frac{[\mathrm{Biomass}] \cdot MW_{SUC}}{10^6}$$
$$\frac{d[\mathrm{FOR}]}{dt} = \nu_{PFL} - \nu_{FOR,transport} - 107.59 \cdot \mu - \mu \cdot [\mathrm{FOR}]$$
$$\frac{d[\mathrm{ACE}]}{dt} = \nu_{PTACK} + 581.01 \cdot \mu - \nu_{ACE,transport} - \mu \cdot [\mathrm{ACE}]$$
$$\frac{d[\mathrm{ETH}]}{dt} = \nu_{ADH} - \nu_{ETH,transport} - \mu \cdot [\mathrm{ETH}]$$
$$\frac{d[\mathrm{LAC}]}{dt} = \nu_{LDH} - \nu_{LAC,transport} - \mu \cdot [\mathrm{LAC}]$$
$$\frac{d[\mathrm{SUC}]}{dt} = \nu_{FRD} + 1040.71 \cdot \mu - \nu_{SUC,transport} - \mu \cdot [\mathrm{SUC}]$$
$$\frac{d[\mathrm{G6P}]}{dt} = \nu_{PTS} - \nu_{PGI} - 600.28 \cdot \mu - \mu \cdot [\mathrm{G6P}]$$
$$\frac{d[\mathrm{F6P}]}{dt} = \nu_{PGI} - \nu_{PFK} - 466.42 \cdot \mu - \mu \cdot [\mathrm{F6P}]$$
$$\frac{d[\mathrm{FBP}]}{dt} = \nu_{PFK} - \nu_{FBA} - \mu \cdot [\mathrm{FBP}]$$
$$\frac{d[\mathrm{GAP}]}{dt} = 2 \cdot \nu_{FBA} - \nu_{GDH} - 459.27 \cdot \mu - \mu \cdot [\mathrm{GAP}]$$
$$\frac{d[\mathrm{BPG}]}{dt} = \nu_{GDH} - \nu_{PGK} - \mu \cdot [\mathrm{BPG}]$$
$$\frac{d[\mathrm{3PG}]}{dt} = \nu_{PGK} - \nu_{ENO} - 1717.48 \cdot \mu - \mu \cdot [\mathrm{3PG}]$$
$$\frac{d[\mathrm{PEP}]}{dt} = \nu_{ENO} + \nu_{PCK} - \nu_{PYK} - \nu_{PPC} - \nu_{PTS} - 810.19 \cdot \mu - \mu \cdot [\mathrm{PEP}]$$
$$\frac{d[\mathrm{PYR}]}{dt} = \nu_{PTS} + \nu_{PYK} - \nu_{PFL} - \nu_{LDH} - \nu_{PYR,transport} - 2784.13 \cdot \mu - \mu \cdot [\mathrm{PYR}]$$

$$\frac{d[\mathrm{AcCoA}]}{dt} = v_{PFL} - v_{PTACK} - v_{ALDH} - v_{CSICD} - 3856.57 \cdot \mu - \mu \cdot [\mathrm{AcCoA}]$$
$$\frac{d[\mathrm{ACTLD}]}{dt} = v_{ALDH} - v_{ADH} - \mu \cdot [\mathrm{ALDH}]$$
$$\frac{d[\mathrm{OAA}]}{dt} = v_{PPC} - v_{MDH} - v_{CSICD} - v_{PCK} - 2924.97 \cdot \mu - \mu \cdot [\mathrm{OAA}]$$
$$\frac{d[\mathrm{AKG}]}{dt} = v_{CSICD} - 1075.32 \cdot \mu - \mu \cdot [\mathrm{AKG}]$$
$$\frac{d[\mathrm{FUM}]}{dt} = v_{MDH} - v_{FRD} - \mu \cdot [\mathrm{FUM}]$$
$$\frac{d[\mathrm{ATP}]}{dt} = v_{PTACK} + 0.75 \cdot v_{FRD} + v_{PGK} + v_{PYK} - v_{PFK} - v_{PCK} - v_{NGAM} - v_{ADK} - 53107.60 \cdot \mu - \mu \cdot [\mathrm{ATP}]$$
$$\frac{d[\mathrm{ADP}]}{dt} = v_{PFK} + v_{PCK} + v_{NGAM} + 2 \cdot v_{ADK} - v_{PTACK} - 0.75 \cdot v_{FRD} - v_{PGK} - v_{PYK} - 49739.5 \cdot \mu - \mu \cdot [\mathrm{ADP}]$$
$$\frac{d[\mathrm{NADH}]}{dt} = v_{GDH} + v_{CSICD} - v_{ADH} - v_{ALDH} - v_{LDH} - v_{FRD} - v_{MDH} - 14889.30 \cdot \mu - \mu \cdot [\mathrm{NADH}]$$

The following equations show the conservation rules of the conserved moieties contained in the model. Accordingly, algebraic equations were used to balance the species [ADP], [NAD], and [CoA].

$[\mathrm{ATP}] + [\mathrm{ADP}] + [\mathrm{AMP}] = 2.70$ µmol/gDW (Measured in this study)
$[\mathrm{NAD}] + [\mathrm{NADH}] = 2.78$ µmol/gDW (Chassagnole *et al*, 2002)
$[\mathrm{AcCoA}] + [\mathrm{CoA}] = 3.49$ µmol/gDW (Park *et al*, 2016)

1.3 Reactions and rate laws

PTS reaction

$$\mathrm{Glc_{ex}} + \mathrm{PEP} \rightarrow \mathrm{PYR} + \mathrm{G6P}$$

The glucose phosphotransferase system (PTS) is the main glucose uptake mechanism in *E. coli*. The overall reaction is modeled using Michaelis-Menten kinetics. Inhibition terms for PYR and G6P reflect reduced uptake when PYR and G6P accumulate.

$$v_{PTS} = v_{max,PTS} \cdot \frac{\frac{[\mathrm{PEP}]}{k_{PTS,PEP}} \cdot \frac{[\mathrm{Glc_{ex}}]}{k_{PTS,Glc}} \cdot \left(1 - \frac{\frac{[\mathrm{G6P}]\,[\mathrm{PYR}]}{[\mathrm{PEP}]\,[\mathrm{Glcex}]}}{k_{PTS,eq}}\right)}{1 + \frac{[\mathrm{PEP}]}{k_{PTS,PEP}} + \frac{[\mathrm{Glc_{ex}}]}{k_{PTS,Glc}} + \frac{[\mathrm{PYR}]}{k_{PTS,PYR}} + \left(\frac{[\mathrm{G6P}]}{k_{PTS,G6P}}\right)^{n_{PTS,G6P}}}$$

Parameter	Value	Unit	Reference
$v_{max,PTS}$	12.53	[µmol/gDW/s]	**
$k_{PTS,eq}$	12	[-]	(Rohwer *et al*, 2000)
$k_{PTS,PEP}$	0.531	[µmol/gDW]	(Rohwer *et al*, 2000)
$k_{PTS,Glc}$	0.0345	[µmol/gDW]	(Rohwer *et al*, 2000)
$k_{PTS,G6P}$	1.0625	[µmol/gDW]	Bettenbrock
$k_{PTS,PYR}$	3.54	[µmol/gDW]	(Rohwer *et al*, 2000)
$n_{PTS,G6P}$	2.21	[-]	**

**** Here and in the following ** means that the parameter has been estimated in this study.**

PGI reaction

$$\mathrm{G6P} \leftrightarrow \mathrm{F6P}$$

The isomerization of G6P into F6P is described using Michaelis-Menten kinetics as in (Peskov *et al*, 2012). As observed in (Ogawa *et al*, 2007), PEP acts as inhibitor for the reaction.

$$v_{PGI} = v_{max,PGI} \cdot \frac{\frac{[\mathrm{G6P}]}{k_{PGI,G6P}} \cdot \left(1 - \frac{[\mathrm{F6P}]}{[\mathrm{G6P}]}{k_{PGI,EQ}}\right)}{1 + \frac{[\mathrm{G6P}]}{k_{PGI,G6P}} + \frac{[\mathrm{F6P}]}{k_{PGI,F6P}} + \frac{[\mathrm{PEP}]}{k_{PGI,PEP}}}$$

Parameter	Value	Unit	Reference
$v_{max,PGI}$	20	[µmol/gDW/s]	**
$k_{PGI,EQ}$	0.3	[-]	(Noor *et al*, 2013)
$k_{PGI,G6P}$	0.31	[µmol/gDW]	(Ogawa *et al*, 2007)
$k_{PGI,F6P}$	0.293	[µmol/gDW]	(Ishii *et al*, 2007)
$k_{PGI,PEP}$	0.46	[µmol/gDW]	(Ogawa *et al*, 2007)

PFK reaction

$$\mathrm{F6P} + \mathrm{ATP} \rightarrow \mathrm{FBP} + \mathrm{ADP}$$

The PFK reaction catalyzes the phosphorylation of F6P and is a key enzyme for the glycolysis pathway and regulated in different ways. As reported in (Peskov *et al*, 2008),

- a complex of ATP with magnesium ions ($ATPMg^{2+}$) acts as real substrate for PFK;
- the reaction rate depends sigmoidal on the F6P concentration;
- PFK is allosterically activated by ADP and inhibited by PEP.

To keep track of all these effects, a modular convenience kinetics is used (Liebermeister *et al*, 2010). For simplicity, ATP and ADP are directly used to avoid the introduction of the magnesium complexes.

$$v_{PFK} = v_{max,PFK} \cdot \left(\frac{[\mathrm{ADP}]}{k_{PFK,a,ADP} + [\mathrm{ADP}]}\right) \cdot \left(\frac{k_{PFK,i,PEP}}{k_{PFK,i,PEP} + [\mathrm{PEP}]}\right)^{n_{PFK,i,PEP}} \cdot \left(\frac{\frac{[\mathrm{ATP}]}{k_{PFK,ATP}} \cdot \left(\frac{[\mathrm{F6P}]}{k_{PFK,F6P}}\right)^{n_{PFK,F6P}} \cdot \left(1 - \frac{[\mathrm{ADP}]\,[\mathrm{FBP}]}{[\mathrm{ATP}]\,[\mathrm{F6P}]^{n_{PFK,F6P}}}{k_{PFK,EQ}}\right)}{\left(1 + \frac{[\mathrm{ATP}]}{k_{PFK,ATP}}\right) \cdot \left(1 + \frac{[\mathrm{F6P}]}{k_{PFK,F6P}}\right)^{n_{PFK,F6P}} + \left(1 + \frac{[\mathrm{FBP}]}{k_{PFK,FBP}}\right) \cdot \left(1 + \frac{[\mathrm{ADP}]}{k_{PFK,ADP}}\right) - 1} \right)$$

Parameter	Value	Unit	Reference
$v_{max,PFK}$	22.74	[µmol/gDW/s]	**
$k_{PFK,EQ}$	1300	[-]	(Noor *et al*, 2013)
$k_{PFK,ATP}$	1.03	[µmol/gDW]	**
$k_{PFK,F6P}$	0.0531	[µmol/gDW]	(Berger & Evans, 1991)
$k_{PFK,FBP}$	5	[µmol/gDW]	**
$k_{PFK,ADP}$	4.28	[µmol/gDW]	**
$k_{PFK,a,ADP}$	0.2886	[µmol/gDW]	**

$k_{PFK,i,PEP}$	3.45	[µmol/gDW]	(Ogawa *et al*, 2007)
$n_{PFK,i,PEP}$	2.61	[-]	**
$n_{PFK,F6P}$	1.9	[-]	(Ishii *et al*, 2007)

FBA reaction

$$\mathrm{FBP} \leftrightarrow 2\ \mathrm{GAP}$$

This reaction lumps together the FBA and TPI (triose-phosphate isomerase) reactions. According to (Ogawa *et al*, 2007), an inhibition term for PEP was introduced.

$$v_{FBA} = \frac{v_{max,FBA,F} \cdot \frac{[\mathrm{FBP}]}{k_{FBA,FBP}} \cdot \left(1 - \frac{[\mathrm{GAP}]^2}{[\mathrm{FBP}]}{k_{FBA,EQ}}\right)}{1 + \frac{[\mathrm{FBP}]}{k_{FBA,FBP}} + \left(\frac{[\mathrm{GAP}]}{k_{FBA,GAP}}\right)^2 + \left(\frac{[\mathrm{PEP}]}{k_{FBA,PEP}}\right)^{n_{FBA,PEP}}}$$

Parameter	Value	Unit	Reference
$v_{max,FBA,F}$	25	[µmol/gDW/s]	**
$k_{FBA,FBP}$	40	[µmol/gDW]	**
$k_{FBA,GAP}$	16.6	[µmol/gDW]	Kotte 2012
$k_{FBA,PEP}$	0.89	[µmol/gDW]	**
$n_{FBA,PEP}$	2.89	[-]	**
$k_{FBA,EQ}$	0.177	[µmol/gDW]	(Babul *et al*, 1993)

GDH reaction

$$\mathrm{GAP} + \mathrm{NAD} \leftrightarrow \mathrm{BPG} + \mathrm{NADH}$$

This reaction is described using convenience kinetic.

$$v_{GDH} = v_{max,GDH} \cdot \frac{\frac{[\mathrm{GAP}]}{k_{GDH,GAP}} \cdot \frac{[\mathrm{NAD}]}{k_{GDH,NAD}} \cdot \left(1 - \frac{[\mathrm{BPG}]\ [\mathrm{NADH}]}{[\mathrm{GAP}][\mathrm{NAD}]}{k_{GDH,EQ}}\right)}{\left(1 + \frac{[\mathrm{NAD}]}{k_{GDH,NAD}} + \frac{[\mathrm{NADH}]}{k_{GDH,NADH}}\right) \cdot \left(1 + \frac{[\mathrm{GAP}]}{k_{GDH,GAP}} + \frac{[\mathrm{BPG}]}{k_{GDH,BPG}}\right)}$$

Parameter	Value	Unit	Reference
$v_{max,GDH,F}$	20.86	[µmol/gDW/s]	**
$k_{GDH,EQ}$	1679	[-]	Noor
$k_{GDH,GAP}$	0.0983	[µmol/gDW]	**
$k_{GDH,NAD}$	0.0194	[µmol/gDW]	(Millard *et al*, 2017; Wright *et al*, 1995)
$k_{GDH,BPG}$	0.354	[µmol/gDW]	(Lambeir *et al*, 1991)
$k_{GDH,NADH}$	6.549	[µmol/gDW]	(Millard *et al*, 2017)

PGK reaction

$$\mathrm{BPG} + \mathrm{ADP} \leftrightarrow 3\mathrm{PG} + \mathrm{ATP}$$

This reaction is modeled using a Random Bi-Bi kinetics as used in (Peskov *et al*, 2012).

$$v_{PGK} = v_{max,PGK} \frac{\frac{[\mathrm{BPG}]\cdot[\mathrm{ADP}]}{k_{PGK,BPG}\cdot k_{PGK,ADP}} \cdot \left(1 - \frac{\frac{[\mathrm{ATP}]\cdot[\mathrm{3PG}]}{[\mathrm{BPG}]\cdot[\mathrm{ADP}]}}{k_{PGK,EQ}}\right)}{Den_{PGK}}$$

$$Den_{PGK} = 1 + \frac{[\mathrm{ADP}]}{k_{PGK,ADP}} + \frac{[\mathrm{BPG}]}{k_{PGK,BPG}} + \frac{[\mathrm{BPG}]\cdot[\mathrm{ADP}]}{k_{PGK,BPG}\cdot k_{PGK,ADP}} + \frac{[\mathrm{3PG}]}{k_{PGK,3PG}} + \frac{[\mathrm{ATP}]}{k_{PGK,ATP}} + \frac{[\mathrm{3PG}]\cdot[\mathrm{ATP}]}{k_{PGK,ATP}\cdot k_{PGK,3PG}}$$

Parameter	Value	Unit	Reference
$v_{max,PGK}$	28.9	[µmol/gDW/s]	**
$k_{PGK,EQ}$	2700	[-]	(Noor *et al*, 2013)
$k_{PGK,BPG}$	0.3186	[µmol/gDW]	Kuntz 1982
$k_{PGK,ADP}$	0.0122	[µmol/gDW]	**
$k_{PGK,3PG}$	2.265	[µmol/gDW]	Kuntz 1982
$k_{PGK,ATP}$	2.1996	[µmol/gDW]	**

ENO reaction

$$\mathrm{3PG} \leftrightarrow \mathrm{PEP}$$

This reaction lumps together the reactions of 2,3-bisphosphoglycerate phosphoglycerate mutase and of enolase and its kinetics is described using reversible Michaelis-Menten kinetics.

$$v_{ENO} = v_{max,ENO} \cdot \frac{\frac{[\mathrm{3PG}]}{k_{ENO,3PG}} \cdot \left(1 - \frac{\frac{[PEP]}{[3PG]}}{k_{ENO,EQ}}\right)}{1 + \frac{[\mathrm{3PG}]}{k_{ENO,3PG}} + \frac{[\mathrm{PEP}]}{k_{ENO,PEP}}}$$

Parameter	Value	Unit	Reference
$v_{max,ENO}$	32.12	[µmol/gDW/s]	**
$k_{ENO,EQ}$	4.7	[-]	(Noor *et al*, 2013)
$k_{ENO,3PG}$	1.94	[µmol/gDW]	(Watabe & Freese, 1979)
$k_{ENO,PEP}$	0.177	[µmol/gDW]	Spring 1971

PYK reaction

$$\mathrm{PEP} + \mathrm{ADP} \rightarrow \mathrm{PYR} + \mathrm{ATP}$$

It has been observed that the pyruvate kinase reaction is allosterically activated by FBP and AMP and inhibited by ATP (Iwakura *et al*, 1979; Wohl & Markus, 1972) DOI 10.1016/0005-2744(77)90353-9 . The reaction is modeled using a common modular convenience kinetics (Liebermeister & Klipp, 2006).

$$v_{PYK} = v_{max,PYK} \cdot \left(\frac{[\mathrm{FBP}]}{[\mathrm{FBP}] + k_{PYK,a,FBP}}\right)^{n_{PYK,a,FBP}} \cdot \left(\frac{k_{PYK,i,ATP}}{[\mathrm{ATP}] + k_{PYK,i,ATP}}\right) \cdot \left(\frac{[\mathrm{AMP}]}{[\mathrm{AMP}] + k_{PYK,a,AMP}}\right)^{n_{PYK,a,AMP}} \cdot \left(\frac{\frac{[\mathrm{PEP}]}{k_{PYK,PEP}}^{n_{PYK,PEP}} \cdot \frac{[\mathrm{ADP}]}{k_{PYK,ADP}} \cdot \left(1 - \frac{[\mathrm{PYR}] \cdot [\mathrm{ATP}]}{[\mathrm{PEP}]^{n_{PYK,PEP}} [\mathrm{ADP}]} / k_{PYK,EQ}\right)}{\left(1 + \frac{[\mathrm{PEP}]}{k_{PYK,PEP}}\right)^{n_{PYK,PEP}} \cdot \left(1 + \frac{[\mathrm{ADP}]}{k_{PYK,ADP}}\right) + \left(1 + \frac{[\mathrm{PYR}]}{k_{PYK,PYR}}\right) \cdot \left(1 + \frac{[\mathrm{ATP}]}{k_{PYK,ATP}}\right) - 1} \right)$$

Parameter	Value	Unit	Reference
$v_{max,PYK}$	10.2	[µmol/gDW/s]	**
$k_{PYK,EQ}$	24000	[-]	(Noor *et al*, 2013)
$k_{PYK,PEP}$	0.177	[µmol/gDW]	Malcovati 69 DOI: 10.1016/0005-2744(69)90417-312)
$n_{PYK,PEP}$	1.05		Speranza 1990 10.1111/j.1432-1033.1990.tb19178.x
$k_{PYK,ADP}$	0.0027	[µmol/gDW]	**
$k_{PYK,PYR}$	0.3154	[µmol/gDW]	**
$k_{PYK,ATP}$	0.5357	[µmol/gDW]	**
$k_{PYK,a,FBP}$	5.28	[µmol/gDW]	**
$k_{PYK,i,ATP}$	22.5	[µmol/gDW]	(Chassagnole *et al*, 2002)
$n_{PYK,a,FBP}$	1.3	[-]	**
$k_{PYK,a,AMP}$	0.002		**

PFL reaction

$$\mathrm{PYR} + \mathrm{CoA} \leftrightarrow \mathrm{FOR} + \mathrm{AcCoA}$$

The PFL reaction is present in *E. coli* only under anaerobic conditions and is a key fermentation reaction. The reaction is modeled using Ping-Pong kinetics (as formerly used in (Knappe & Sawers, 1990)).

$$v_{PFL} = v_{max,PFL,F} \cdot \frac{\left(\frac{[\mathrm{PYR}] \cdot [\mathrm{CoA}]}{k_{PFL,CoA} \cdot k_{PFL,PYR}} \cdot \left(1 - \frac{[\mathrm{FOR}] \cdot [\mathrm{AcCoA}]}{[\mathrm{PYR}] \cdot [\mathrm{CoA}]} / k_{PFL,EQ}\right)\right)}{Den_{PFL}}$$

$$Den_{PFL} = \frac{[\mathrm{PYR}] \cdot [\mathrm{CoA}]}{k_{PFL,CoA} \cdot k_{PFL,PYR}} + \frac{[\mathrm{PYR}]}{k_{PFL,PYR}} + \frac{[\mathrm{CoA}]}{k_{PFL,CoA}} \cdot \left(1 + \frac{[\mathrm{AcCoA}]}{k_{PFL,i,AcCoA}}\right) + \frac{1}{k_{PFL,AcCoA} \cdot k_{PFL,FOR}} \cdot \left(k_{PFL,AcCoA} \cdot [\mathrm{FOR}] \cdot \left(1 + \frac{[\mathrm{PYR}]}{k_{PFL,i,PYR}}\right) + [\mathrm{AcCoA}] \cdot \left(k_{PFL,FOR} + [\mathrm{FOR}]\right)\right)$$

Parameter	Value	Unit	Reference

$v_{max,PFL,F}$	20.1	[µmol/gDW/s]	(Matsuoka & Kurata, 2017)
$k_{PFL,EQ}$	3000	[-]	(Noor *et al*, 2013)
$k_{PFL,PYR}$	0.4518	[µmol/gDW]	**
$k_{PFL,CoA}$	0.0124	[µmol/gDW]	Knappe 1974
$k_{PFL,AcCoA\cdot}$	0.0903	[µmol/gDW]	Knappe 1974
$k_{PFL,FOR}$	43.36	[µmol/gDW]	Knappe 19742)
$k_{PFL,i,AcCoA}$	1.51	[µmol/gDW]	**
$k_{PFL,i,PYR}$	1	[µmol/gDW]	**

PTACK reaction

$$\mathrm{AcCoA} + \mathrm{ADP} \rightarrow \mathrm{ACE} + \mathrm{ATP} + \mathrm{CoA}$$

The PTACK reaction lumps together the phosphate acetyltransferase and acetate kinase reactions and is modeled using a direct binding convenience kinetics. As reported in (Campos-Bermudez *et al*, 2010), PEP and PYR are activators for the reaction and ATP acts as inhibitor.

$$v_{PTACK} = v_{max,PTACK} \cdot \left(\frac{[\mathrm{PYR}]}{k_{PTACK,PYR} + [\mathrm{PYR}]}\right) \cdot \left(\frac{[\mathrm{PEP}]}{k_{PTACK,PEP} + [\mathrm{PEP}]}\right) \cdot \left(\frac{k_{PTACK,i,ATP}}{k_{PTACK,i,ATP} + [\mathrm{ATP}]}\right) \cdot \left(\frac{\left(\frac{[\mathrm{AcCoA}]}{k_{PTACK,AcCoA}}\right)^{n_{PTACK,AcCoA}} \cdot \frac{[\mathrm{ADP}]}{k_{PTACK,ADP}} \left(1 - \frac{ACEin \cdot CoA\,ATP}{ACoA^{n_{PTACK,AcCoA}} \cdot ADP} / k_{PTACK,EQ}\right)}{\left(1 + \frac{[\mathrm{AcCoA}]}{k_{PTACK,AcCoA}}\right)^{n_{PTACK,AcCoA}} \cdot \left(1 + \frac{[\mathrm{ADP}]}{k_{PTACK,ADP}}\right) + \left(1 + \frac{[\mathrm{ATP}]}{k_{PTACK,ATP}}\right) \cdot \left(1 + \frac{[\mathrm{CoA}]}{k_{PTACK,CoA}}\right) \cdot \left(1 + \frac{[ACEin]}{k_{PTACK,ACEin}}\right) - 1} \right)$$

Parameter	Value	Unit	Reference
$v_{max,PTACK}$	23.53	[µmol/gDW/s]	**
$k_{PTACK,EQ}$	4790	[-]	Murabito 2014
$k_{PTACK,AcCoA}$	0.0794	[µmol/gDW]	(Campos-Bermudez *et al*, 2010)
$k_{PTACK,ADP}$	0.3161	[µmol/gDW]	**
$k_{PTACK,ATP}$	0.1239	[µmol/gDW]	Fox & Rosemann 1985
$k_{PTACK,CoA}$	0.118	[µmol/gDW]	(Campos-Bermudez *et al*, 2010)
$k_{PTACK,i,ATP}$	4.56	[µmol/gDW]	**
$k_{PTACK,PYR}$	0.0261	[µmol/gDW]	**
$k_{PTACK,PEP}$	0.25	[µmol/gDW]	** in accordance with the value of 0.5 mM of (Campos-Bermudez *et al*, 2010)
$n_{PTACK,AcCoA}$	4	[-]	**
$k_{PTACK,ACEin}$	12.39	[µmol/gCDW]	Fox & Rosemann 1985

ALDH reaction

$$\mathrm{AcCoA} + \mathrm{NADH} \leftrightarrow \mathrm{ACTLD} + \mathrm{CoA} + \mathrm{NAD}$$

The acetaldehyde-CoA dehydrogenase reaction is modeled using an ordered Bi-Bi rate law (Wratten & Cleland, 1963).

$$v_{ALDH} = \frac{v_{max,ALDH} \cdot \left(\frac{[\mathrm{AcCoA}] \cdot [\mathrm{NADH}]}{k_{ALDH,i,AcCoA} \cdot k_{ALDH,NADH}} \left(1 - \frac{[\mathrm{ACTLD}] \cdot [\mathrm{CoA}]}{[\mathrm{AcCoA}] \cdot [\mathrm{NADH}]} \right) \right)}{Den_{ALDH}}$$

$$Den_{ALDH} = 1 + \frac{[\mathrm{AcCoA}]}{k_{ALDH,i,AcCoA}} + \frac{[\mathrm{AcCoA}] \cdot [\mathrm{NADH}]}{k_{ALDH,i,AcCoA} \cdot k_{ALDH,NADH}} + \frac{[\mathrm{CoA}]}{k_{ALDH,i,CoA}} + \frac{[\mathrm{ACTLD}] \cdot [\mathrm{CoA}]}{k_{ALDH,i,CoA} \cdot k_{ALDH,ACTLD}}$$

Parameter	Value	Unit	Reference
$v_{max,ALDH}$	295	[µmol/gDW/s]	**
$k_{ALDH,EQ}$	0.273	[-]	**
$k_{ALDH,i,AcCoA}$	0.012	[µmol/gDW]	(Shone & Fromm, 1981)
$k_{ALDH,NADH}$	0.1	[µmol/gDW]	**
$k_{ALDH,i,CoA}$	0.014	[µmol/gDW]	(Cintolesi *et al*, 2012)
$k_{ALDH,ACTLD}$	17.7	[µmol/gDW]	(Shone & Fromm, 1981)

ADH reaction

$$\mathrm{ACTLD} + \mathrm{NADH} \leftrightarrow \mathrm{ETH} + \mathrm{CoA} + \mathrm{NAD}$$

The alcohol dehydrogenase reaction is modeled using ordered Bi-Bi rate equation (Wratten & Cleland, 1963) :

$$v_{ADH} = \frac{v_{max,ADH} \cdot \left(\frac{[\mathrm{ACTLD}] \cdot [\mathrm{NADH}]}{k_{ADH,i,ACTLD} \cdot k_{ADH,NADH}} \left(1 - \frac{[\mathrm{ETH}] \cdot [\mathrm{NAD}]}{[\mathrm{ACTLD}] \cdot [\mathrm{NADH}]} \right) \right)}{Den_{ADH}}$$

$$Den_{ADH} = 1 + \frac{[\mathrm{ACTLD}]}{k_{ADH,i,ACTLD}} + \frac{[\mathrm{ACTLD}] \cdot [\mathrm{NADH}]}{k_{ADH,i,ACTLD} \cdot k_{ADH,NADH}} + \frac{[\mathrm{NAD}]}{k_{ADH,i,NAD}} + \frac{[\mathrm{NAD}] \cdot [\mathrm{ETH}]}{k_{ADH,i,NAD} \cdot k_{ADH,ETH}}$$

Parameter	Value	Unit	Reference
$v_{max,ADH}$	18	[µmol/gDW/s]	**
$k_{ADH,EQ}$	1500	[-]	(Noor *et al*, 2013)
$k_{ADH,i,ACTLD}$	0.0531	[µmol/gDW]	(Hoefnagel *et al*, 2002)
$k_{ADH,NADH}$	0.172	[µmol/gDW]	**
$k_{ADH,i,NAD}$	0.142	[µmol/gDW]	(Matsuoka & Kurata, 2017)
$k_{ADH,ETH}$	1.77	[µmol/gDW]	(Hoefnagel *et al*, 2002)

LDH reaction

$$\mathrm{PYR} + \mathrm{NADH} \rightarrow \mathrm{LAC} + \mathrm{NAD}$$

The reaction is modeled using a common modular rate law (liebermeister 2010) including the homotropic effect of PYR and NADH reported in MTarmyN OKaplan.

$$v_{LDH} = v_{max,LDH} \cdot \frac{\left(\frac{[\mathrm{PYR}]}{k_{LDH,PYR}}\right)^{n_{LDH,PYR}} \left(\frac{[\mathrm{NADH}]}{k_{LDH,NADH}}\right)^{n_{LDH,NADH}} \left(\frac{[\mathrm{LACin}][\mathrm{NAD}]}{[\mathrm{PYR}]^{n_{LDH,PYR}}\,[\mathrm{NADH}]^{n_{LDH,NADH}}}{k_{LDH,EQ}}\right)}{\left(1+\frac{[\mathrm{PYR}]}{k_{LDH,PYR}}\right)^{n_{LDH,PYR}} \left(1+\frac{[\mathrm{NADH}]}{k_{LDH,NADH}}\right)^{n_{LDH,NADH}} + \left(1+\frac{[\mathrm{NAD}]}{k_{LDH,NAH}}\right)\left(1+\frac{[\mathrm{LACin}]}{k_{LDH,LACin}}\right) - 1}$$

Parameter	Value	Unit	Reference
$v_{max,LDH}$	11	[µmol/gCDW/s]	**
$k_{LDH,PYR}$	12.74	[µmol/gCDW]	MTarmyN OKaplan
$n_{LDH,PYR}$	1.2	[-]	MTarmyN OKaplan
$k_{LDH,NADH}$	0.004	[µmol/gCDW]	**
$n_{LDH,NADH}$	1	[-]	MTarmyN OKaplan
$k_{LDH,EQ}$	14000	[-]	(Noor *et al*, 2013)
$k_{LDH,LAC}$	7.84	[µmol/gCDW]	** (Tarmy and Kaplan do not report LACd to have any product inhibition effect in the reaction.)
$k_{LDH,NAD}$	0.4425	[µmol/gCDW]	Tarmy and Kaplan

CSICD reaction

$$\mathrm{AcCoA} + \mathrm{NAD} + \mathrm{OAA} \leftrightarrow \mathrm{AKG} + \mathrm{NADH} + \mathrm{CoA} + \mathrm{CO_2}$$

This reaction lumps all steps from AcCoA to AKG (see also legend of Scheme S1). Reversible common modular convenience kinetics (liebermeister) is used to describe the reaction. The inhibition of the citrate synthase by AKG and NADH (as observed in 10.1016/0014-5793(83)80873-4) is accounted for in the kinetics.

$$v_{CSICD} = v_{max,CSICD} \cdot \frac{\frac{[\mathrm{AcCoA}]}{k_{CSICD,AcCoA}} \cdot \frac{[\mathrm{OAA}]}{k_{CSICD,OAA}} \frac{[\mathrm{NAD}]}{k_{CSICD,NAD}} \left(1 - \frac{[\mathrm{AKG}][\mathrm{CoA}][\mathrm{NADH}][\mathrm{CO_2}]}{[\mathrm{ACoA}][\mathrm{NAD}][\mathrm{OAA}]\ k_{CSICD,EQ}}\right)}{\left(\left(1+\frac{[\mathrm{AcCoA}]}{k_{CSICD,AcCoA}}\right)\cdot\left(1+\frac{[\mathrm{OAA}]}{k_{CSICD,OAA}}\right)\cdot\left(1+\frac{[\mathrm{NAD}]}{k_{CSICD,NAD}}\right) - 1\right)} \cdot \left(\frac{k_{CSICD,i,NADH}}{k_{CSICD,i,NADH} + [\mathrm{NADH}]}\right) \cdot \left(\frac{k_{CSICD,i,AKG}}{k_{CSICD,i,AKG} + [\mathrm{AKG}]}\right)^{n_{CSICD,i,AKG}}$$

Parameter	Value	Unit	Reference
$v_{max,CSICD}$	1.956	[µmol/gDW/s]	**
$k_{CSICD,EQ}$	6.2	[-]	**
$k_{CSICD,AcCoA}$	0.2124	[µmol/gDW]	(Anderson & Duckworth, 1988)
$k_{CSICD,NAD}$	0.067	[µmol/gDW]	**

$k_{CSICD,OAA}$	0.046	[µmol/gDW]	**
$k_{CSICD,AKG}$	0.628	[µmol/gDW]	(Kotte *et al*, 2010)
$n_{CSICD,AKG}$	4	[-]	**
$k_{CSICD,i,NADH}$	0.7		Danson 1973 10.1042/bj1350513

PCK reaction

$$\mathrm{OAA} + \mathrm{ATP} \leftrightarrow \mathrm{PEP} + \mathrm{CO_2} + \mathrm{ADP}$$

This reaction catalyzes the carboxylation of oxaloacetate to PEP under consumption of ATP. Under particular conditions, the reaction can also run in the reverse direction (Zhang *et al*, 2009) accompanied with the production of ATP. A simplified Random Bi Ter mechanism is used to model the kinetics as in (Peskov *et al*, 2012):

$$v_{PCK} = \frac{v_{max,PCK} \cdot \left(\frac{[\mathrm{OAA}] \cdot [\mathrm{ATP}]}{k_{PCK,OAA} \cdot k_{PCK,ATP}} \cdot \left(1 - \frac{[\mathrm{PEP}] \cdot [\mathrm{CO_2}] \cdot [\mathrm{ADP}]}{[\mathrm{OAA}] \cdot [\mathrm{ATP}]} \right) \right)}{PCK_{DEN}}$$

$$PCK_{DEN} = 1 + \frac{[\mathrm{ATP}]}{k_{PCK,ATP}} + \frac{[\mathrm{OAA}]}{k_{PCK,OAA}} + \frac{[\mathrm{OAA}] \cdot [\mathrm{ATP}]}{k_{PCK,OAA} \cdot k_{PCK,ATP}} + \left(\frac{[\mathrm{CO_2}]}{k_{PCK,CO_2}} + \frac{[\mathrm{PEP}]}{k_{PCK,PEP}} + \frac{[\mathrm{ADP}]}{k_{PCK,ADP}} + \frac{[\mathrm{PEP}] \cdot [\mathrm{CO_2}]}{k_{PCK,PEP} \cdot k_{PCK,CO_2}} + \frac{[\mathrm{CO_2}] \cdot [\mathrm{ADP}]}{k_{PCK,CO_2} \cdot k_{PCK,ADP}} + \frac{[\mathrm{PEP}] \cdot [\mathrm{ADP}]}{k_{PCK,PEP} \cdot k_{PCK,ADP}} + \frac{[\mathrm{PEP}] \cdot [\mathrm{ADP}] \cdot [\mathrm{CO_2}]}{k_{PCK,PEP} \cdot k_{PCK,ADP} \cdot k_{PCK,CO_2}} \right)$$

Parameter	Value	Unit	Reference
$v_{max,PCK}$	0.0513	[µmol/gDW/s]	**
$k_{PCK,EQ}$	1.88	[µmol/gDW]	(Peskov *et al*, 2012)
$k_{PCK,OAA}$	1.18	[µmol/gDW]	(Krebs & Bridger, 1980)
$k_{PCK,ATP}$	0.1062	[µmol/gDW]	(Krebs & Bridger, 1980)
k_{PCK,CO_2}	2.571	[µmol/gDW]	**
$k_{PCK,PEP}$	0.885	[µmol/gDW]	(Krebs & Bridger, 1980)
$k_{PCK,ADP}$	0.0885	[µmol/gDW]	(Krebs & Bridger, 1980)
$[\mathrm{CO_2}]$	2.478	[µmol/gDW]	(Millard *et al*, 2017)

PPC reaction

$$\mathrm{PEP} + \mathrm{CO_2} \rightarrow \mathrm{OAA}$$

The anaplerotic PPC reaction catalyzes the carboxylation of PEP into OAA. A sigmoidal response to PEP has been observed (Wohl & Markus, 1972), and the reaction is modeled using direct binding convenience kinetics (Liebeerm 2010). Activation from ACoA and FBP (Izi 10.1016/0014-5793(81)80531-5) and inhibition of by FUM (Yano 10.1111/j.1432-1033.1997.t01-1-00074.x) are take into account.

$$r_{PPC} = v_{max,PPC} \cdot \frac{\left(\frac{[\mathrm{PEP}]}{k_{PPC,PEP}}\right)^{n_{PPC,PEP}} \cdot \frac{[\mathrm{CO_2}]}{k_{PPC,CO_2}} \cdot \left(1 - \frac{[\mathrm{OAA}]}{[\mathrm{PEP}]^{n_{PPC,PEP}}[\mathrm{CO_2}]}{k_{PPC,EQ}}\right)}{\left(1 + \left(\frac{[\mathrm{PEP}]}{k_{PPC,PEP}}\right)^{n_{PPC,PEP}} + \frac{[\mathrm{CO_2}]}{k_{PPC,CO_2}} + \frac{[\mathrm{OAA}]}{k_{PPC,OAA}}\right)} \cdot \left(\frac{\mathrm{ACoA}}{k_{PPC,a,ACoA} + \mathrm{ACoA}}\right)^{n_{PPC,a,ACoA}} \cdot \left(\frac{\mathrm{FBP}}{k_{PPC,a,FBP} + \mathrm{FBP}}\right) \cdot \left(\frac{k_{PPC,i,MAL}}{k_{PPC,i,MAL} + \mathrm{MAL}}\right)$$

Parameter	Value	Unit	Reference
$v_{max,PPC}$	3.087	[µmol/gCDW/s]	**
$k_{PPC,PEP}$	0.2655	[µmol/gCDW]	[35] Yano
$k_{PPC,EQ}$	2001	[-]	(Noor *et al*, 2013)
k_{PPC,CO_2}	1.09	[µmol/gCDW]	[36] Kai 1999
$k_{PPC,OAA}$	1.387	[µmol/gCDW]	**
$n_{PPC,PEP}$	4	[-]	Peskov
$k_{PPC,a,ACoA}$	0.7611	[µmol/gCDW]	T.E.Smith 1980 https://doi.org/10.1016/S0021-9258(19)86080-5
$n_{PPC,a,ACoA}$	1.4	Estimated from	T.E.Smith 1980 https://doi.org/10.1016/S0021-9258(19)86080-5
$k_{PPC,a,FBP}$	5.98	[µmol/gCDW]	T.E.Smith 1980 https://doi.org/10.1016/S0021-9258(19)86080-5
$k_{PPC,i,MAL}$	0.2124	[µmol/gCDW]	M Yano 1997 DOI: 10.1111/j.1432-1033.1997.t01-1-00074.x
CO2	2.478	[µmol/gCDW]	fixed

MDH reaction

$$\mathrm{OAA} + \mathrm{NADH} \leftrightarrow \mathrm{FUM} + \mathrm{NAD}$$

This reaction describes the left branch of the TCA cycle under anaerobic conditions, lumping together the malate dehydrogenase and fumarase reactions. The reaction is modeled using ordered Bi-Bi reaction law as observed in DOI: 10.1006/abbi.1995.1397 S K Wright et Al., 1995.

$$v_{MDH} = \frac{v_{max,MDH,F} \cdot \frac{[\mathrm{OAA}] \cdot [\mathrm{NADH}]}{k_{MDH,i,OAA} \cdot k_{MDH,NADH}} \left(1 - \frac{\frac{[\mathrm{MAL}] \cdot [\mathrm{NAD}]}{[\mathrm{OAA}] \cdot [\mathrm{NADH}]}}{k_{MDH,EQ}}\right)}{D_{MDH}}$$

$$D_{MDH} = 1 + \frac{[\mathrm{NADH}] \cdot k_{MDH,OAA}}{k_{MDH,i,OAA} \cdot k_{MDH,NADH}} + \frac{[\mathrm{OAA}]}{k_{MDH,i,OAA}} + \frac{[\mathrm{OAA}] \cdot [\mathrm{NADH}]}{k_{MDH,i,OAA} \cdot k_{MDH,NADH}} + \frac{k_{MDH,NAD} \cdot [\mathrm{OAA}] \cdot [\mathrm{MAL}]}{k_{MDH,MAL} \cdot k_{MDH,i,NAD} \cdot k_{MDH,i,OAA}} + \frac{[\mathrm{NAD}] \cdot [\mathrm{MAL}]}{k_{MDH,MAL} \cdot k_{MDH,i,NAD}} + \frac{[\mathrm{NADH}] \cdot [\mathrm{NAD}] \cdot [\mathrm{MAL}]}{k_{MDH,MAL} \cdot k_{MDH,i,NAD} \cdot k_{MDHi,NADH}} + \frac{[\mathrm{OAA}] \cdot [\mathrm{NADH}] \cdot [\mathrm{MAL}]}{k_{MDH,i,MAL} \cdot k_{MDH,i,OAA} \cdot k_{MDH,NADH}} + \frac{k_{MDH,OAA} \cdot [\mathrm{NADH}] \cdot [\mathrm{NAD}]}{k_{MDH,i,NAD} \cdot k_{MDH,i,OAA} \cdot k_{MDH,NADH}} + \frac{k_{MDH,NAD} \cdot [\mathrm{MAL}]}{k_{MDH,MAL} \cdot k_{MDH,i,NAD}} + \frac{[\mathrm{NAD}]}{k_{MDH,i,NAD}}$$

Parameter	Value	Unit	Reference
$v_{max,MDH,F}$	2.75	[µmol/gCDW/s]	**
$k_{MDH,EQ}$	4.4e+04	[-]	(Noor *et al*, 2013)
$k_{MDH,OAA}$	0.09912	[µmol/gCDW]	DOI: 10.1074/jbc.274.17.11761 Kim99a
$k_{MDH,NADH}$	0.10797	[µmol/gCDW] 0.02832	DOI: 10.1016/S0006-3495(95)80430-3 Muslin 95
$k_{MDH,MAL}$	0.1699	[µmol/gCDW]	DOI:https://doi.org/10.1074/jbc.M114.595363 Anastassia A. Vorobieva 2014
$k_{MDH,NAD}$	0.16638	[µmol/gCDW]	DOI:https://doi.org/10.1074/jbc.M114.595363 Anastassia A. Vorobieva 2014
$k_{MDH,i,OAA}$	0.0354	[µmol/gCDW]	https://doi.org/10.1006/abbi.1995.1397 Wright 1995
$k_{MDH,i,NAD}$	0.041	[µmol/gCDW]	Millard
$k_{MDH,i,MAL}$	0.8	[µmol/gCDW]	**
$k_{MDH,i,NADH}$	0.02832	[µmol/gCDW]	https://doi.org/10.1006/abbi.1995.1397 Wright 1995

FRD reaction

$$\mathrm{FUM} + \mathrm{NADH} + 0.75\ \mathrm{ADP} \rightarrow \mathrm{SUC} + \mathrm{NAD} + 0.75\ \mathrm{ATP}$$

This lumped reaction describes ATP synthesis via fumarate reduction. The first step is the conversion of fumarate into succinate via fumarate reductase in which menaquinol is oxidized to menaquinone. In *E. coli*, menaquinol is regenerated by the oxidation of NADH via an NADH dehydrogenase, that in turn is linked to proton translocation from cytoplasm to periplasm which then enables ATP production via ATP synthase. In the cumulated stoichiometry of this reaction in the model, the menaquinol pool is not explicitly modeled and the effects on NADH and ATP directly taken into account. The reaction is modeled using Michaelis-Menten kinetics. As reported in (Maklashina *et al*, 2006), OAA acts as an inhibitor for the reaction.

$$r_{FRD} = v_{max,FRD} \cdot \frac{\frac{[FUM]}{k_{FRD,FUM}} \cdot \frac{[\mathrm{NADH}]}{k_{FRD,NADH}} \cdot \left(\frac{[\mathrm{ADP}]}{k_{FRD,ADP}}\right)^{0.75} \cdot \left(1 - \frac{\frac{[SUC][NAD]\,[ATP]^{0.75}}{[FUM][NADH]\,[ADP]^{0.75}}}{k_{FRD,EQ}}\right)}{\left(1 + \frac{[FUM]}{k_{FRD,FUM}} + \frac{[\mathrm{NADH}]}{k_{FRD,NADH}} + \left(\frac{[\mathrm{ADP}]}{k_{FRD,ADP}}\right)^{0.75} + \frac{[\mathrm{OAA}]}{k_{FRD,i,OAA}}\right)}$$

Parameter	Value	Unit	Reference

$v_{max,FRD}$	2.89	[µmol/gDW/s]	**
$k_{FRD,EQ}$	120	[-]	(Noor *et al*, 2013)
$k_{FRD,FUM}$	0.0354	[µmol/gDW]	(Maklashina *et al*, 2006)
$k_{FRD,NADH}$	0.02	[µmol/gDW]	**
$k_{FRD,ADP}$	0.1429	[µmol/gDW]	**
$k_{FRD,OAA}$	0.63	[µmol/gDW]	**

NGAM reaction

$$\mathrm{ATP} \rightarrow \mathrm{ADP}$$

The NGAM reaction models the hydrolysis of ATP into ADP and represents the consumption of ATP for non-growth associated maintenance processes. The reaction is modeled using a hill kinetics. The v_{max} has been chosen to yield a minimum non-growth associated maintenance flux for all strains similar to the one determined experimentally and close to 3.15 mmol (gDW h)$^{-1}$, a value that is often used as reference for NGAM demand of ATP in *E. coli* (Orth *et al*, 2011).

$$v_{ATPM} = v_{max,ATPM} \cdot \frac{[\mathrm{ATP}]^{\,n_{ATPM}}}{k_{ATPM,ATP}^{n_{ATPM}} + [\mathrm{ATP}]^{\,n_{ATPM}}}$$

Parameter	Value	Unit	Reference
$v_{max,ATPM}$	1.2	[µmol/gDW/s]	**
$k_{ATPM,ATP}$	0.008	[µmol/gDW]	**
n_{ATPM}	8	[-]	**

ATPase reaction

$$\mathrm{ATP} \rightarrow \mathrm{ADP}$$

The ATPase reaction describes the hydrolysis of ATP into ADP and is the reaction which is overexpressed in LC, MC and HC strains. When simulating the effect of increasing levels of ATPase in the cell, the $v_{max,ATPase}$ is increased accordingly.

$$v_{ATPase} = v_{max,ATPase} \cdot \frac{[\mathrm{ATP}]^{\,n_{ATPase}}}{k_{ATPase,ATP}^{n_{ATPase}} + [\mathrm{ATP}]^{\,n_{ATPase}}}$$

Parameter	Value	Unit	Reference
$v_{max,ATPase}$	0 - 23	[µmol/gDW/s]	**
$k_{ATPase,ATP}$	0.37	[µmol/gDW]	**
n_{ATPase}	2.38	[-]	**

ADK reaction

$$\mathrm{AMP} + \mathrm{ATP} = 2\,\mathrm{ADP}$$

The adenylate kinase reaction accounts for the conversion of AMP and ATP into ADP. The reaction is modeled as in Millard.

$$v_{ADK} = v_{max,ADK} \cdot \left([\mathrm{AMP}]\,[\mathrm{ATP}] - \frac{[\mathrm{ADP}]^2}{k_{ADK,eq}} \right)$$

Parameter	Value	Unit	Reference

$v_{max,ADK}$	0.4283	[µmol/gCDW/s]	**
$k_{ADK,eq}$	0.9	[-]	Equilibrator

Growth reaction

A biomass synthesis reaction was included in the model to account for growth. This pseudo reaction consumes intracellular precursors (here: PEP, PYR, GAP, ATP, AcCoA, AKG, OAA, NADH, F6P, G6P, 3PG) with the following stoichiometries (metabolite stoichiometries (except biomass) given in µmol):

$$\begin{aligned} 459.27\ \mathrm{GAP} + 810.19\ \mathrm{PEP} + 2784.13\ \mathrm{PYR} + 53107.60\ \mathrm{ATP} + 3856.57\ \mathrm{AcCoA} + 1075.32\ \mathrm{AKG} \\ + 2924.97\ \mathrm{OAA} + 14889.30\ \mathrm{NADH} + 466.42\ \mathrm{F6P} + 600.28\ \mathrm{G6P} + 1717.48\ \mathrm{3PG} \\ + 107.95\ \mathrm{FOR} \\ \rightarrow 1\ gram\ \mathrm{Biomass} + 581.01\ \mathrm{ACE} + 2334.41\ \mathrm{CO_2} + 1040.71\ \mathrm{SUC} + 14889.30\ \mathrm{NAD} \\ + 3856.57\ \mathrm{CoA} + 49739.5\ \mathrm{ADP} \end{aligned}$$

The stoichiometry was obtained by reducing a genome-scale stoichiometric model of *E coli* (iJO1366(Orth *et al*, 2011)) to the core metabolic network shown in Scheme S1 using the NetworkReducer package of *CellNetAnalyzer* (Erdrich *et al*, 2015; Klamt *et al*, 2007) . The stoichiometry obtained with this reduction method accounts implicitly for all carbon precursors and cofactors from the core model needed to build the original building blocks (e.g. amino acids, nucleotides etc.) of the biomass in the genome-scale model. For example, 0.51 mmol alanine is needed (among many other building blocks) in *i*JO1366 for building 1 gram of biomass. Since alanine is synthesized by transamination of pyruvate (pyruvate + glutamate → alanine + oxoglutarate) and since recycling of glutamate from oxoglutarate consumes one NADPH (and one ammonia molecule not considered herein), alanine synthesis is accounted for in the reduced biomass synthesis stoichiometry by consumption of 0.51 mmol pyruvate and 0.51 mmol NADH (as was described earlier, in our model, NADPH is included in the NADH pool). As was mentioned in section 1.1, the cumulated biomass stoichiometry also accounts for consumption of the precursors erythrose-4-phosphate and ribose-5-phosphate in the PPP.

For the kinetics of the growth rate we use a Monod kinetics term for each precursor and cofactor consumed in the biomass stoichiometry given above:

$$\mu = \mu_{max} \cdot \frac{[\mathrm{F6P}]}{k_{g,F6P} + [\mathrm{F6P}]} \cdot \frac{[\mathrm{GAP}]}{k_{g,GAP} + [\mathrm{GAP}]} \cdot \frac{[\mathrm{PEP}]}{k_{g,PEP} + [\mathrm{PEP}]} \cdot \frac{[\mathrm{PYR}]}{k_{g,PYR} + [\mathrm{PYR}]} \cdot \frac{[\mathrm{ATP}]}{k_{g,ATP} + [\mathrm{ATP}]} \cdot \frac{[\mathrm{AcCoA}]}{k_{g,AcCoA} + [\mathrm{AcCoA}]} \cdot \frac{[\mathrm{AKG}]}{k_{g,AKG} + [\mathrm{AKG}]} \cdot \frac{[\mathrm{OAA}]}{k_{g,OAA} + [\mathrm{OAA}]} \cdot \frac{[\mathrm{NADH}]}{k_{g,NADH} + [\mathrm{NADH}]} \cdot \frac{[\mathrm{G6P}]}{k_{g,G6P} + [\mathrm{G6P}]} \cdot \frac{[\mathrm{3PG}]}{k_{g,3PG} + [\mathrm{3PG}]} \cdot \frac{[\mathrm{FOR}]}{k_{g,FOR} + [\mathrm{FOR}]}$$

where μ_{max} represents the maximum growth rate (here in [1/s]).

Parameter	Value	Unit	Reference
μ_{max}	4.25e-04	[1/s]	**
$k_{g,F6P}$	0.15	[µmol/gDW]	**
$k_{g,GAP}$	0.0021	[µmol/gDW]	**
$k_{g,PEP}$	0.075	[µmol/gDW]	**
$k_{g,PYR}$	0.007	[µmol/gDW]	**
$k_{g,ATP}$	1.314	[µmol/gDW]	**
$k_{g,ACoA}$	0.43	[µmol/gDW]	**
$k_{g,AKG}$	4.3e-05	[µmol/gDW]	**
$k_{g,OAA}$	0.00049	[µmol/gDW]	**
$k_{g,NADH}$	7.2e-05	[µmol/gDW]	**

$k_{g,3PG}$	0.018	[µmol/gDW]	**
$k_{g,G6P}$	0.75	[µmol/gDW]	**
$k_{g,FOR}$	1e-04	[µmol/gDW]	**

Export reactions

The reactions describing the export of FOR, LAC, ACE, ETH, PYR and SUC between the cytoplasm and the external environment are modeled using Michaelis-Menten kinetics. The parameters values were chosen to ensure that the transport reactions are no limiting steps to the fermentative fluxes (similarly to (Millard *et al*, 2017)).

Formate transport

$$\mathrm{FOR} \rightarrow \mathrm{FOR}_{ex}$$

$$v_{FOR_{transport}} = v_{max,FOR_{transport}} \frac{[\mathrm{FOR}]}{\left([\mathrm{FOR}] + k_{FOR_{transport}}\right)}$$

Parameter	Value	Unit	Reference
$v_{max,FOR_{transport}}$	100	[µmol/gDW/s]	**
$k_{FOR_{transport}}$	10	[µmol/gDW]	**

Lactate transport

$$\mathrm{LAC} \rightarrow \mathrm{LAC}_{ex}$$

$$v_{LAC_{transport}} = v_{max,LAC_{transport}} \frac{[\mathrm{LAC}]}{\left([\mathrm{LAC}] + k_{LAC_{transport}}\right)}$$

Parameter	Value	Unit	Reference
$v_{max,LAC_{transport}}$,	100	[µmol/gDW/s]	**
$k_{LAC_{transport}}$	10	[µmol/gDW]	**

Acetate transport

$$\mathrm{ACE} \rightarrow \mathrm{ACE}_{\mathrm{ex}}$$

$$v_{ACE_{transport}} = v_{max,ACE_{transport}} \frac{[\mathrm{ACE}]}{\left([\mathrm{ACE}] + k_{ACE_{transport}}\right)}$$

Parameter	Value	Unit	Reference
$v_{max,ACE_{transport}}$	100	[µmol/gDW/s]	**
$k_{ACE_{transport}}$	10	[µmol/gDW]	**

Ethanol transport

$$\mathrm{ETH} \rightarrow \mathrm{ETH}_{ex}$$

$$v_{ETH_{transport}} = v_{max,ETH_{transport}} \frac{[\mathrm{ETH}]}{\left([\mathrm{ETH}] + k_{ETH_{transport}}\right)}$$

Parameter	Value	Unit	Reference
$v_{max,ETH_{transport}}$	100	[µmol/gDW/s]	**
$k_{ETH_{transport}}$	10	[µmol/gDW]	**

Succinate transport

$$\mathrm{SUC} \rightarrow \mathrm{SUC}_{ex}$$

$$v_{SUC_{transport}} = v_{max,SUC_{transport}} \cdot \frac{[\mathrm{SUC}]}{[\mathrm{SUC}] + k_{SUC_{transport}}}$$

Parameter	Value	Unit	Reference
$v_{SUC_{transport},max}$	100	[µmol/gDW/s]	**
$k_{SUC_{transport}}$	10	[µmol/gDW]	**

Fumarate uptake
This reaction was set inactive in all simulations except for a single case, where we tested the effect of supplying fumarate as additional substrate under ATPase HC conditions (see Discussion section in the main text). The reaction is modeled using irreversible Michaelis-Menten kinetics with product inhibition.

$$\mathrm{FUM}_{ex} \rightarrow \mathrm{FUM}$$

$$v_{FUM_{transport}} = v_{max,FUM_{uptake}} \frac{\frac{[\mathrm{FUM}_{ex}]}{k_{FUM_{uptake},FUMex}}}{\left(1 + \frac{[\mathrm{FUM}_{ex}]}{k_{FUM_{uptake},FUMex}} + \frac{[\mathrm{FUM}]}{k_{FUM_{uptake},FUM}}\right)}$$

Parameter	Value	Unit	Reference
$v_{max,FUM_{uptake}}$	0 - 20	[µmol/gDW/s]	**
$k_{FUM_{uptake},FUMex}$	0.1	[g/l]	**
$k_{FUM_{uptake},FUM}$	0.52	[µmol/gDW]	**
$[\mathrm{FUM}_{ex}]$	1	[g/l]	**

1.4 Simulations and reference points

For a direct comparison of simulated and measured rates and concentrations for the different ATPase strains (Figure 3b and 4 in the main document) we determined, for a given strain, the (reference) $v_{max,ATPase}$ value such that the simulated and the measured (steady-state) glucose uptake rate in the respective ATPase strain was identical. This reference point was then chosen to compare the other measured fluxes and the metabolite concentrations for this strain. The determined reference points are as follows for model version 1 (cf. Figure 3b and 4 in main manuscript): (1) WT strain: $v_{max,ATPase}$ = 0 mmol/(gDW h); (2) LC ATPase strain : $v_{max,ATPase}$ = 9.7 mmol/(gDW h); (3) MC ATPase strain: $v_{max,ATPase}$ = 37.1 mmol/(gDW h); and 4) HC ATPase strain: $v_{max,ATPase}$ = 86.4 mmol/(gDW h).

2. Kinetic model version 2

As described in the main text, the first version of the model was able to reproduce the biphasic behavior of the measured exchange fluxes. However, as shown in Figure 4 in the main document, the model failed in predicting major trends of the intracellular metabolite concentrations (in particular, of FBP, PEP and PYR) and no lactate was produced by ATPase HC. To overcome this issue and for the reasons reported in the main text, some modifications have been introduced in model version 2, which are described below. Afterwards, metabolic control analysis was performed with model version 2 to identify potential bottleneck reactions for the glycolytic flux.

2.1 Corrected Rate Laws and Parameters

In the following we describe only changes in the kinetic rate laws and parameters introduced in model version 2 (changes are indicated in bold). All other rate laws, ODEs and parameters are identical to model version 1.

PFL reaction: introduction of a regulation term
A regulation term is introduced for PFL to ensure that it is only active (or expressed) under conditions with sufficiently high ATP concentrations.

$$\mathrm{PYR} + \mathrm{CoA} \leftrightarrow \mathrm{FOR} + \mathrm{AcCoA}$$

$$v_{PFL,modified} = \frac{[\mathbf{ATP}]^{\boldsymbol{n_{rf}}}}{[\mathbf{ATP}]^{\boldsymbol{n_{rf}}} + \boldsymbol{k_{rf}^{n_{rf}}}} \cdot v_{max,PFL,F} \cdot \frac{\left(\frac{[\mathrm{PYR}] \cdot [\mathrm{CoA}]}{k_{PFL,CoA} \cdot k_{PFL,PYR}} \cdot \left(1 - \frac{\frac{[\mathrm{FOR}] \cdot [\mathrm{AcCoA}]}{[\mathrm{PYR}] \cdot [\mathrm{CoA}]}}{k_{PFL,EQ}} \right) \right)}{Den_{PFL}}$$

$$Den_{PFL} = \frac{[\mathrm{PYR}] \cdot [\mathrm{CoA}]}{k_{PFL,CoA} \cdot k_{PFL,PYR}} + \frac{[\mathrm{PYR}]}{k_{PFL,PYR}} + \frac{[\mathrm{CoA}]}{k_{PFL,CoA}} \cdot \left(1 + \frac{[\mathrm{AcCoA}]}{k_{PFL,i,AcCoA}} \right) + \frac{1}{k_{PFL,AcCoA} \cdot k_{PFL,FOR}} \cdot \left(k_{PFL,AcCoA} \cdot [\mathrm{FOR}] \cdot \left(1 + \frac{[\mathrm{PYR}]}{k_{PFL,i,PYR}} \right) + [\mathrm{AcCoA}] \cdot \left(k_{PFL,FOR} + [\mathrm{FOR}] \right) \right)$$

Parameter	Value	Unit	Reference
$v_{max,PFL,F}$	20.1	[µmol/gDW/s]	(Matsuoka & Kurata, 2017)
$k_{PFL,EQ}$	3000	[-]	(Noor *et al*, 2013)
$k_{PFL,PYR}$	0.4518	[µmol/gDW]	**
$k_{PFL,CoA}$	0.0124	[µmol/gDW]	Knappe 1974
$k_{PFL,AcCoA\cdot}$	0.0903	[µmol/gDW]	Knappe 1974
$k_{PFL,FOR}$	43.36	[µmol/gDW]	Knappe 19742)
$k_{PFL,i,AcCoA}$	1.51	[µmol/gDW]	**
$k_{PFL,i,PYR}$	1	[µmol/gDW]	**
$\boldsymbol{k_{rf}}$	0.94	[µmol/gDW]	**
$\boldsymbol{n_{rf}}$	2.8	[-]	**

PYK reaction: introduction of a PYR dependent inhibition term
An inhibition term depending on the abundance of PYR has been introduced to reflect decreased activity of PYK in presence of high amounts of PYR.

$$\mathrm{PEP} + \mathrm{ADP} \rightarrow \mathrm{PYR} + \mathrm{ATP}$$

$$v_{PYK,modified} = v_{max,PYK} \cdot \left(\frac{\frac{[\mathrm{PEP}]}{k_{PYK,PEP}} \cdot \frac{[\mathrm{ADP}]}{k_{PYK,ADP}}}{\left(1 + \frac{[\mathrm{PEP}]}{k_{PYK,PEP}} \right) \cdot \left(1 + \frac{[\mathrm{ADP}]}{k_{PYK,ADP}} \right) + \left(1 + \frac{[\mathrm{PYR}]}{k_{PYK,PYR}} \right) \cdot \left(1 + \frac{[\mathrm{ATP}]}{k_{PYK,ATP}} \right) - 1} \right) \cdot \left(\frac{[\mathrm{FBP}]}{[\mathrm{FBP}] + k_{PYK,a,FBP}} \right)^{n_{PYK,a,FBP}} \cdot \left(\frac{k_{PYK,i,ATP}}{[\mathrm{ATP}] + k_{PYK,i,ATP}} \right) \cdot \left(\left(\frac{\boldsymbol{k_{PYK,i,PYR}}}{[\mathbf{PYR}] + \boldsymbol{k_{PYK,i,PYR,}}} \right)^{\boldsymbol{n_{PYK,i,PYR}}} \right)$$

Parameter	Value	Unit	Reference
$v_{max,PYK}$	14	[µmol/gDW/s]	**
$k_{PYK,PEP}$	0.177	[µmol/gDW]	(Peskov *et al*, 2012)
$k_{PYK,ADP}$	0.0228	[µmol/gDW]	**
$k_{PYK,PYR}$	0.3154	[µmol/gDW]	**
$\boldsymbol{k_{PYK,ATP}}$	**5**	[µmol/gDW]	**
$k_{PYK,a,FBP}$	15	[µmol/gDW]	**
$k_{PYK,i,ATP}$	22.5	[µmol/gDW]	(Chassagnole *et al*, 2002)
$\boldsymbol{n_{PYK,a,FBP}}$	**1.6**	[-]	**
$\boldsymbol{k_{PYK,i,PYR}}$	**7**	[µmol/gDW]	**
$\boldsymbol{n_{PYK,i,PYR}}$	**4**	[-]	**

$$v_{PYK} = v_{max,PYK} \cdot \left(\frac{[\mathrm{FBP}]}{[\mathrm{FBP}] + k_{PYK,a,FBP}}\right)^{n_{PYK,a,FBP}} \cdot \left(\frac{k_{PYK,i,ATP}}{[\mathrm{ATP}] + k_{PYK,i,ATP}}\right) \cdot \left(\frac{[\mathrm{AMP}]}{[\mathrm{AMP}] + k_{PYK,a,AMP}}\right)^{n_{PYK,a,AMP}} \cdot \left(\left(\frac{\boldsymbol{k_{PYK,i,PYR}}}{[\mathbf{PYR}] + \boldsymbol{k_{PYK,i,PYR,}}}\right)^{\boldsymbol{n_{PYK,i,PYR}}}\right) \cdot \left(\frac{\frac{[\mathrm{PEP}]}{k_{PYK,PEP}}^{n_{PYK,PEP}} \cdot \frac{[\mathrm{ADP}]}{k_{PYK,ADP}} \cdot \left(1 - \frac{[\mathrm{PYR}] \cdot [\mathrm{ATP}]}{[\mathrm{PEP}]^{n_{PYK,PEP}}\,[\mathrm{ADP}]}{k_{PYK,EQ}}\right)}{\left(1 + \frac{[\mathrm{PEP}]}{k_{PYK,PEP}}\right)^{n_{PYK,PEP}} \cdot \left(1 + \frac{[\mathrm{ADP}]}{k_{PYK,ADP}}\right) + \left(1 + \frac{[\mathrm{PYR}]}{k_{PYK,PYR}}\right) \cdot \left(1 + \frac{[\mathrm{ATP}]}{k_{PYK,ATP}}\right) - 1}\right)$$

Parameter	Value	Unit	Reference
$v_{max,PYK}$	15.64	[µmol/gDW/s]	**
$k_{PYK,EQ}$	24000	[-]	(Noor *et al*, 2013)
$k_{PYK,PEP}$	0.177	[µmol/gDW]	Malcovati 69 DOI: 10.1016/0005-2744(69)90417-312)
$n_{PYK,PEP}$	1.05		Speranza 1990 10.1111/j.1432-1033.1990.tb19178.x
$k_{PYK,ADP}$	0.0027	[µmol/gDW]	**
$k_{PYK,PYR}$	0.3154	[µmol/gDW]	**
$k_{PYK,ATP}$	0.5357	[µmol/gDW]	**
$k_{PYK,a,FBP}$	5.28	[µmol/gDW]	**
$k_{PYK,i,ATP}$	22.5	[µmol/gDW]	(Chassagnole *et al*, 2002)
$n_{PYK,a,FBP}$	1.3	[-]	**
$k_{PYK,a,AMP}$	0.002		**
$\boldsymbol{k_{PYK,i,PYR}}$	**6.8**	[µmol/gDW]	**
$\boldsymbol{n_{PYK,i,PYR}}$	**2.82**	[-]	**

ATPase reaction: parameter modification

$$v_{ATPase} = v_{max,ATPase} \cdot \frac{[\mathrm{ATP}]^{\,n_{ATPase}}}{k_{ATPase,ATP}^{n_{ATPase}} + [\mathrm{ATP}]^{\,n_{ATPase}}}$$

Parameter	Value	Unit	Reference
$v_{max,ATPase}$	0 - 23	[µmol/gDW/s]	**
$\boldsymbol{k_{ATPase,ATP}}$	0.73	[µmol/gDW]	**
$\boldsymbol{n_{ATPase}}$	3.75	[-]	**

2.2 Simulations and reference points

As for kinetic model version 1, we chose (reference) $v_{max,ATPase}$ values for the different strains such that the simulated and the measured (steady-state) glucose uptake rate in the respective ATPase strain was identical. The reference points for model version 2 (cf. Figure 4 in main manuscript) changed slightly to: (1) WT strain: $v_{max,ATPase}$ = 0 mmol/(gDW h) (this represents the non-growth associated ATP maintenance demand without ATPase expression); (2) LC ATPase strain: $v_{max,ATPase}$ = 10.36 mmol/(gDW h); (3) MC ATPase strain: $v_{max,ATPase}$ = 39.31 mmol/(gDW h); and (4) HC ATPase strain: $v_{max,ATPase}$ = 82.94 mmol/(gDW h).

References

Anderson DH, Duckworth HW (1988) *In vitro* mutagenesis of *Escherichia coli* citrate synthase to clarify the locations of ligand binding sites. *J Biol Chem* 263: 2163-2169

Arriaga D, Soler J, Cadenas E (1982) Influence of pH on the allosteric properties of lactate dehydrogenase activity of *Phycomyces blakesleeanus*. *Biochem J* 203: 393-400

Babul J, Clifton D, Kretschmer M, Fraenkel DG (1993) Glucose metabolism in *Escherichia coli* and the effect of increased amount of aldolase. *Biochemistry* 32: 4685-92

Balzer S, Kucharova V, Megerle J, Lale R, Brautaset T, Valla S (2013) A comparative analysis of the properties of regulated promoter systems commonly used for recombinant gene expression in *Escherichia coli*. *Microb Cell Fact* 12: 26

Berger SA, Evans PR (1991) Steady-state fluorescence of *Escherichia coli* phosphofructokinase reveals a regulatory role for ATP. *Biochemistry* 30: 8477-8480

Blattner FR, Plunkett III G, Bloch CA, Perna NT, Burland V, Riley M, Collado-Vides J, Glasner JD, Rode CK, Mayhew GF, Gregor J, Davis NW, Kirkpatrick HA, Goeden MA, Rose DJ, Mau B, Shao Y (1997) The Complete Genome Sequence of *Escherichia coli* K-12. *Science* 277: 1453

Busto F, Arriaga D, Soler J (1984) The kinetic mechanism of pyruvate reduction by lactate dehydrogenase from *Phycomyces blakesleeanus*. *Int J Biochem* 16: 171-176

Campos-Bermudez VA, Bologna FP, Andreo CS, Drincovich MF (2010) Functional dissection of *Escherichia coli* phosphotransacetylase structural domains and analysis of key compounds involved in activity regulation. *FEBS J* 277: 1957-1966

Chassagnole C, Noisommit-Rizzi N, Schmid JW, Mauch K, Reuss M (2002) Dynamic modeling of the central carbon metabolism of *Escherichia coli*. *Biotechnol Bioeng* 79: 53-73

Cintolesi A, Clomburg JM, Rigou V, Zygourakis K, Gonzalez R (2012) Quantitative analysis of the fermentative metabolism of glycerol in *Escherichia coli*. *Biotechnol Bioeng* 109: 187-198

Erdrich P, Steuer R, Klamt S (2015) An algorithm for the reduction of genome-scale metabolic network models to meaningful core models. *BMC Syst Biol* 9: 48

Fox DK, Roseman S (1986) Isolation and characterization of homogeneous acetate kinase from *Salmonella typhimurium* and *Escherichia coli*. *J Biol Chem* 261: 13487-13497

Hoefnagel MHN, Starrenburg MJC, Martens DE, Hugenholtz J, Kleerebezem M, Van S, II, Bongers R, Westerhoff HV, Snoep JL (2002) Metabolic engineering of lactic acid bacteria, the combined approach: kinetic modelling, metabolic control and experimental analysis. *Microbiology (Reading, Engl)* 148: 1003-1013

Hoops S, Sahle S, Gauges R, Lee C, Pahle J, Simus N, Singhal M, Xu L, Mendes P, Kummer U (2006) COPASI—a COmplex PAthway SImulator. *Bioinformatics* 22: 3067-3074

Ishii N, Suga Y, Hagiya A, Watanabe H, Mori H, Yoshino M, Tomita M (2007) Dynamic simulation of an *in vitro* multi-enzyme system. *FEBS Lett* 581: 413-420

Iwakura M, Hattori J, Arita Y, Tokushige M, Katsuki H (1979) Studies on regulatory functions of malic enzymes. VI. Purification and molecular properties of NADP-linked malic enzyme from *Escherichia coli* W. *J Biochem* 85: 1355-1365

Kai Y, Matsumura H, Inoue T, Terada K, Nagara Y, Yoshinaga T, Kihara A, Tsumura K, Izui K (1999) Three-dimensional structure of phosphoenolpyruvate carboxylase: a proposed mechanism for allosteric inhibition. *Proc Natl Acad Sci USA* 96: 823-828

Klamt S, Saez-Rodriguez J, Gilles ED (2007) Structural and functional analysis of cellular networks with *CellNetAnalyzer*. *BMC Syst Biol* 1: 2

Knappe J, Sawers G (1990) A radical-chemical route to acetyl-CoA: the anaerobically induced pyruvate formate-lyase system of Escherichia coli. *FEMS Microbiol Rev* 6: 383-98

Koebmann BJ, Westerhoff HV, Snoep JL, Nilsson D, Jensen PR (2002) The Glycolytic Flux in *Escherichia coli* Is Controlled by the Demand for ATP. *J Bacteriol* 184: 3909-3916

Kotte O, Zaugg JB, Heinemann M (2010) Bacterial adaptation through distributed sensing of metabolic fluxes. *Mol Syst Biol* 6: 355

Krebs A, Bridger WA (1980) The kinetic properties of phosphoenolpyruvate carboxykinase of *Escherichia coli*. *Can J Biochem* 58: 309-318

Lambeir AM, Loiseau AM, Kuntz DA, Vellieux FM, Michels PA, Opperdoes FR (1991) The cytosolic and glycosomal glyceraldehyde-3-phosphate dehydrogenase from *Trypanosoma brucei*. Kinetic properties and comparison with homologous enzymes. *Eur J Biochem* 198: 429-435

Liebermeister W, Klipp E (2006) Bringing metabolic networks to life: convenience rate law and thermodynamic constraints. *Theor Biol Med Model* 3: 41

Liebermeister W, Uhlendorf J, Klipp E (2010) Modular rate laws for enzymatic reactions: thermodynamics, elasticities and implementation. *Bioinformatics* 26: 1528-1534

Lutz R, Bujard H (1997) Independent and tight regulation of transcriptional units in *Escherichia coli* via the LacR/O, the TetR/O and AraC/I_1-I_2 regulatory elements. *Nucleic Acids Res* 25: 1203-1210

Maklashina E, Iverson TM, Sher Y, Kotlyar V, Andréll J, Mirza O, Hudson JM, Armstrong FA, Rothery RA, Weiner JH, Cecchini G (2006) Fumarate reductase and succinate oxidase activity of *Escherichia coli* complex II homologs are perturbed differently by mutation of the flavin binding domain. *J Biol Chem* 281: 11357-11365

Matsuoka Y, Kurata H (2017) Modeling and simulation of the redox regulation of the metabolism in *Escherichia coli* at different oxygen concentrations. *Biotechnol Biofuels* 10: 183

Millard P, Smallbone K, Mendes P (2017) Metabolic regulation is sufficient for global and robust coordination of glucose uptake, catabolism, energy production and growth in *Escherichia coli*. *PLOS Comput Biol* 13: e1005396

Muslin EH, Li D, Stevens FJ, Donnelly M, Schiffer M, Anderson LE (1995) Engineering a domain-locking disulfide into a bacterial malate dehydrogenase produces a redox-sensitive enzyme. *Biophys J* 68: 2218-2223

Noor E, Haraldsdottir HS, Milo R, Fleming RM (2013) Consistent estimation of Gibbs energy using component contributions. *PLOS Comput Biol* 9: e1003098

Ogawa T, Mori H, Tomita M, Yoshino M (2007) Inhibitory effect of phosphoenolpyruvate on glycolytic enzymes in *Escherichia coli*. *Res Microbiol* 158: 159-163

Orth JD, Conrad TM, Na J, Lerman JA, Nam H, Feist AM, Palsson BO (2011) A comprehensive genome-scale reconstruction of *Escherichia coli* metabolism. *Mol Syst Biol* 7: 535

Park JO, Rubin SA, Xu Y-F, Amador-Noguez D, Fan J, Shlomi T, Rabinowitz JD (2016) Metabolite concentrations, fluxes and free energies imply efficient enzyme usage. *Nat Chem Biol* 12: 482-489

Peskov K, Goryanin I, Demin O (2008) Kinetic model of phosphofructokinase-1 from *Escherichia coli*. *J Bioinform Comput Biol* 6: 843-867

Peskov K, Mogilevskaya E, Demin O (2012) Kinetic modelling of central carbon metabolism in *Escherichia coli*. *FEBS J* 279: 3374-3385

Rohwer JM, Meadow ND, Roseman S, Westerhoff HV, Postma PW (2000) Understanding glucose transport by the bacterial phosphoenolpyruvate:glycose phosphotransferase system on the basis of kinetic measurements in vitro. *J Biol Chem* 275: 34909-34921

Sauro MH (2019) *Systems Biology: An Introduction to Metabolic Control Analysis*. Ambrosius Publishing, USA

Shone CC, Fromm HJ (1981) Steady-state and pre-steady-state kinetics of coenzyme A linked aldehyde dehydrogenase from *Escherichia coli*. *Biochemistry* 20: 7494-7501

Switzer A, Burchell L, McQuail J, Wigneshweraraj S (2020) The Adaptive Response to Long-Term Nitrogen Starvation in *Escherichia coli* Requires the Breakdown of Allantoin. *J Bacteriol* 202: e0017220

Taymaz-Nikerel H, van Gulik WM, Heijnen JJ (2011) *Escherichia coli* responds with a rapid and large change in growth rate upon a shift from glucose-limited to glucose-excess conditions. *Metab Eng* 13: 307-318

Usuda Y, Nishio Y, Iwatani S, van Dien SJ, Imaizumi A, Shimbo K, Kageyama N, Iwahata D, Miyano H, Matsui K (2010) Dynamic modeling of *Escherichia coli* metabolic and regulatory systems for amino-acid production. *J Biotechnol*: 17-30

Watabe K, Freese E (1979) Purification and properties of the manganese-dependent phosphoglycerate mutase of *Bacillus subtilis*. *J Bacteriol* 137: 773-778

Wohl RC, Markus G (1972) Phosphoenolpyruvate carboxylase of *Escherichia coli*. Purification and some properties. *J Biol Chem* 247: 5785-5792

Wratten CC, Cleland WW (1963) Product Inhibition Studies on Yeast and Liver Alcohol Dehydrogenases*. *Biochemistry* 2: 935-941

Wright SK, Zhao FJ, Rardin J, Milbrandt J, Helton M, Furumo NC (1995) Mechanistic studies on malate dehydrogenase from *Escherichia coli*. *Arch Biochem Biophys* 321: 289-296

Yano M, Terada K, Umiji K, Izui K (1995) Catalytic role of an arginine residue in the highly conserved and unique sequence of phosphoenolpyruvate carboxylase. *J Biochem* 117: 1196-1200

Zhang X, Jantama K, Moore JC, Jarboe LR, Shanmugam KT, Ingram LO (2009) Metabolic evolution of energy-conserving pathways for succinate production in *Escherichia coli*. *Proc Natl Acad Sci USA* 106: 20180-20185